CRUICKSHANK, D. W. J. (1949). *Acta Cryst.* **2**, 65–82.
DERNIER, P. D. (1970). *J. Phys. Chem. Solids*, **31**, 2569–2575.
DWIGGINS, C. W. (1975). *Acta Cryst.* A**31**, 395–396.
FLACK, H. D. & VINCENT, M. G. (1978). *Acta Cryst.* A**34**, 489–491.
FUKAMACHI, T. (1971). Tech. Rep. B12, Institute for Solid State Physics, Univ. of Tokyo.
GOODENOUGH, J. B. (1960). *Phys. Rev.* **117**, 1442–1451.
GOODENOUGH, J. B. (1970). *Proceedings of the Tenth International Conference of Physics of Semiconductors*, edited by S. D. KELLER, J. C. HENSEL & F. STERN, pp. 304–310. US Atomic Energy Commission.
GOODENOUGH, J. B. (1971). *Prog. Solid State Chem.* **5**, 145–399.
International Tables for X-ray Crystallography (1974). Vol. IV. Birmingham: Kynoch Press.
PREWITT, C. T., SHANNON, R. D., ROGERS, D. B. & SLEIGHT, A. W. (1969). *Inorg. Chem.* **8**, 1985–1993.
REES, B. (1976). *Acta Cryst.* A**32**, 483–488.
REES, B. (1978). *Acta Cryst.* A**34**, 254–256.
REES, B. & MITSCHLER, A. (1976). *J. Am. Chem. Soc.* **98**, 7918–7924.
RICE, C. E. & ROBINSON, W. R. (1977). *Acta Cryst.* B**33**, 1342–1348.
ROBINSON, W. R. (1974). *J. Solid State Chem.* **9**, 255–260.
ROBINSON, W. R. (1975). *Acta Cryst.* B**31**, 1153–1160.
STAUDENMANN, J.-L., COPPENS, P. & MÜLLER, J. (1976). *Solid State Commun.* **19**, 29–33.
THORNLEY, F. R. & NELMES, R. J. (1974). *Acta Cryst.* A**30**, 748–757.
VAN ZANDT, L. L., HONIG, J. M. & GOODENOUGH, J. B. (1968). *J. Appl. Phys.* **39**, 594–595.
VINCENT, M. G. & FLACK, H. D. (1979). *Acta Cryst.* A**35**, 78–82.
VINCENT, M. G., YVON, K. & ASHKENAZI, J. (1980). *Acta Cryst.* A**36**, 808–813.
XRAY System (1976). Tech. Rep. TR-446. Computer Science Center, Univ. of Maryland, College Park, Maryland.

Acta Cryst. (1980). A**36**, 808–813

Electron-Density Studies of Metal–Metal Bonds. II.* The Deformation Density of V_2O_3 at 295 K

BY M. G. VINCENT† AND K. YVON

Laboratoire de Cristallographie aux Rayons X, Université de Genève, 24, Quai Ernest Ansermet, CH-1211 Genève 4, Switzerland

AND J. ASHKENAZI

Departement de Physique de la Matière Condensée, Université de Genève, 32, Boulevard d'Yvoy, CH-1211 Genève 4, Switzerland

(*Received* 24 *January* 1980; *accepted* 21 *March* 1980)

Abstract

The charge-density distribution in V_2O_3 differs from that in Ti_2O_3 mainly with respect to the deformation of the metal atoms. The V atoms show a positive deformation of up to 0·1 e Å^{-3} perpendicular to **c** in a plane containing three nearest V-atom sites across the edges of the surrounding O-atom octahedra, and a negative deformation of up to 0·3 e Å^{-3} parallel to **c** between the nearest V-atom site across the faces of the O-atom octahedra. These observations are in accordance with theoretical band-structure calculations and confirm the existence of an e_π metal–metal bond which is directed across the common edges of the metal-centred O-atom octahedra.

Introduction

According to a study of the variation in the c/a ratio in corundum-type oxides (Goodenough, 1963, 1970, 1971; Prewitt, Shannon, Rogers & Sleight, 1969; McWhan, Rice & Remeika, 1969) and theoretical calculations (Ashkenazi & Weger, 1976; Ashkenazi & Chuchem, 1975; Castellani, Natoli & Ranninger, 1978), the metal–metal bonding in V_2O_3 is distinctly different from that in Ti_2O_3. Whereas the metal atoms in Ti_2O_3 interact mainly along the c direction through common faces of the O-atom octahedra, they interact in V_2O_3 mainly in directions perpendicular to the c direction through common edges of the O-atom octahedra (see metal-atom sites V, V′ and V″ in Fig. 1). In a previous article (Vincent, Yvon, Grüttner & Ashkenazi, 1980; hereafter referred to as VYGA), we have presented an experimentally determined electron-density map for Ti_2O_3 which confirms the existence of a

* Part I: Vincent, Yvon, Grüttner & Ashkenazi (1980).

† Present address: Biozentrum der Universität Basel, Klingelbergstrasse 70, CH-4056 Basel, Switzerland.

0567-7394/80/050808-06$01.00

Ti—Ti bond along **c**. In the present study we report on the electron-density distribution in V_2O_3 and compare the bonding features found with those predicted by theory.

Experimental

The experimental procedures adopted in this work and certain features of the refinements were identical or similar to those in the study of Ti_2O_3 (VYGA). Therefore, to obviate a large amount of repetition, this section is restricted to reporting the salient points of the experiment.

A spherical crystal of V_2O_3 of mean radius 79(3) μm was selected from a batch of ground fragments crushed from a large single crystal. An analysis of the effects of non-sphericity on intensity errors (Vincent & Flack, 1979) indicated that the specimen could be approximated to a true sphere with no loss of accuracy.

A hemisphere of X-ray intensities was collected with graphite-monochromated Ag $K\alpha$ radiation ($\lambda = 0{\cdot}5608$ Å) on a four-circle diffractometer in the ω–2θ scan mode out to a limit of 1·43 Å^{-1} in sin θ/λ. The stability of the instrument was monitored by measuring three reference reflections at intervals of 100 min. Variations in the intensities were no greater than 1·3%.

After pre-processing, the intensities were reduced to a set of F values on a common scale corrected for absorption (Dwiggins, 1975) and the usual geometrical factors. Of the 4486 measured reflections, 3547 were classed as observed with $I > 3\sigma(I)$. The latter were used in the calculation of secondary extinction corrections through a weighted least-squares refinement (Becker & Coppens, 1974, 1975) with a modified version of the XRAY System's (1976) *CRYLSQ*. $1/\sigma^2(F)$ weights were used in the refinement and a scale factor and atomic positional and anisotropic thermal parameters were allowed to vary simultaneously with the extinction parameters. Scattering factors for neutral atoms were taken from Fukamachi (1971) and anomalous dispersion terms from *International Tables for X-ray Crystallography* (1974).

Like Ti_2O_3, extinction effects could be best described as Lorentzian type I with the Thornley & Nelmes (1974) form for the angular distribution. T values were determined by the method of Flack & Vincent (1978). Refinement converged at $R(F) = 1{\cdot}6\%$ [$R_w(F) = 2{\cdot}2\%$, $S = 1{\cdot}93$]. The largest correction term implied a reduction in intensity of 44% for the $12\bar{1}0$ reflection.

After applying the extinction corrections to the data, equivalent reflections were averaged and new e.s.d.'s calculated in the same manner as for Ti_2O_3. The data set reduced to 808 independent reflections of which 648 were classified as observed. The internal consistency factor between equivalent reflections was 1.4% in intensity. A further refinement on the observed data converged at $R(F) = 1{\cdot}2\%$ [$R_w(F) = 1{\cdot}1\%$, $S = 1{\cdot}63$].

High-angle refinements were carried out at minimum sin θ/λ cut-offs of 0·65, 0·7, 0·8, 0·9 and 1·0 Å^{-1} with the observed reflections. For similar reasons to those discussed in VYGA, the atomic positional and thermal parameters derived from the 0·65 Å^{-1} cut-off refinement were chosen for the calculation of deformation maps. This refinement converged at $R(F) = 1{\cdot}1\%$ [$R_w(F) = 0{\cdot}8\%$, $S = 0{\cdot}97$] for 570 contributing reflections. The results are given in Table 1 with other relevant information.*

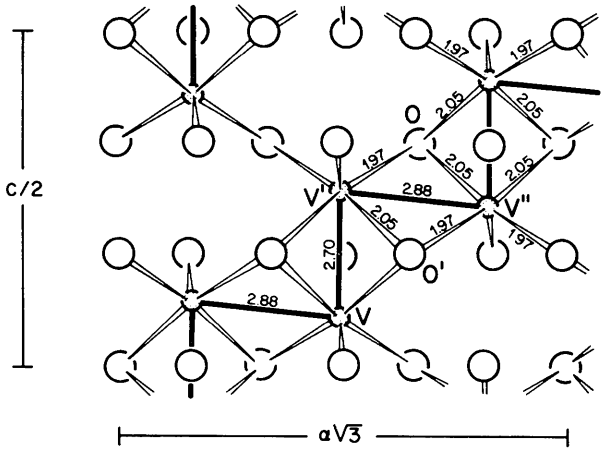

Fig. 1. A projection of the V_2O_3 structure on the $(11\bar{2}0)$ plane. Bond lengths in Å are given to three significant figures.

* Lists of structure factors have been deposited with the British Library Lending Division as Supplementary Publication No. SUP 35174 (8 pp.). Copies may be obtained through The Executive Secretary, International Union of Crystallography, 5 Abbey Square, Chester CH1 2HU, England.

Table 1. *Crystal data for* V_2O_3

For brevity, only the values of the independent, refineable parameters are reported. E.s.d.'s are given in parentheses.

Space group $R\bar{3}c$ (Hexagonal axes)		Positional and thermal parameters‡ V in 12(*c*)	
a	4·9515 (3) Å†	z	0·34629 (1)
c	14·003 (1)	U_{33}	0·00382 (2)
		U_{12}	0·00211 (1)
Extinction parameters ($\times 10^{-4}$)		O in 18(*e*)	
Z_{11}	18·3 (8)		
Z_{22}	31 (1)	x	0·31180 (7)
Z_{33}	9·4 (7)	U_{11}	0·00501 (6)
Z_{12}	−22·0 (8)	U_{33}	0·00557 (6)
Z_{13}	3·3 (6)	U_{12}	0·00281 (4)
Z_{23}	−0·8 (8)	U_{13}	0·00065 (3)
μ(Ag $K\alpha$)	4·467 mm^{-1}		
μR	0·353	scale factor‡	3·713 (6)

† Cell parameters from Dernier (1970).
‡ Obtained from high-angle refinement (see text).

Deformation and error maps

Deformation-density maps were computed in sections with the 73 observed reflections lying in the range $0{\cdot}0 < \sin\theta/\lambda < 0{\cdot}65$ Å^{-1}. A scale factor of 3·752 (6) was determined for this region by least squares, refining on this parameter alone. The bonding features did not significantly change with the inclusion of high-order reflections.

Errors in the deformation density were estimated by the method proposed by Rees (1976, 1978) with a modified version of his program *SIGRHO*. The term $\sigma_{\text{model}}(k)/k$ (Rees, 1978) was estimated to be 0·002. The average error in the observed electron density ρ_o calculated from Cruickshank's (1949) formula was 0·043 e Å^{-3}.

Results and discussion

The deformation-density sections of primary interest with respect to the metal–metal bonding are those parallel to **c**, which contain the metal-atom sites V, V′ and V″, and that perpendicular to **c** which bisects the 2·88 Å bond between the metal-atom sites V′ and V″ at $z = \frac{1}{3}$ (Fig. 1). As can be seen from the maps shown in Fig. 2, the section parallel to **c** contains regions of positive deformation density which concentrate into relatively weak elongated maxima at the metal-atom sites and into relatively strong, irregularly shaped maxima between the metal-atom sites. The weak maxima at the metal-atom sites are connected by a weak electron bridge along [11$\bar{2}$0] and are separated by ribbons of deep negative wells running along [0001]. In the section perpendicular to **c** those maxima have the shape of a three-leaf clover which is centred on the metal-atom site (Fig. 2*b*). Interestingly, the electron-density lobes are not pointing toward the nearest metal-atom sites but are directed away from them by about 30° in such a way that they bisect the angle between the projections of the three 2·05 Å V—O bonds (see dotted lines in Fig. 2*b*).

Clearly, the negative wells in Fig. 2(*a*) and the three-leaf clover-shaped maxima in Fig. 2(*b*) represent a deformation of the V atoms which can be associated with the anticipated metal–metal bonds across the edges of the O-atom octahedra. The deformation density along the V—V′ and V′—V″ bond axes and the corresponding error curves are represented in Fig. 3. One can recognize the deep negative well of about −0·3 e Å^{-3} between the V and V′ atoms sharing a common face, and the weak positive electron bridge between the V′ and V″ atoms sharing a common edge of the O-atom octahedra. Although the error estimates indicate that the electron bridge along the latter bond axis is hardly significant (indeed, the residual positive density at the V sites can only be interpreted as an

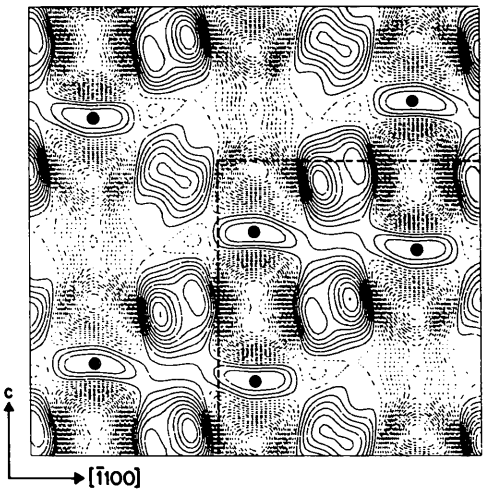

(*a*)

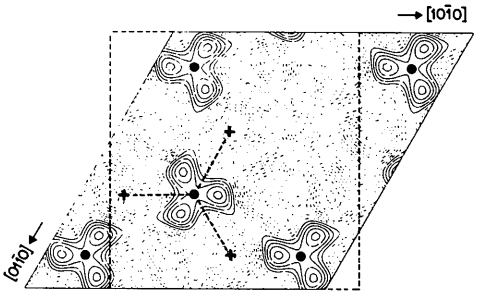

(*b*)

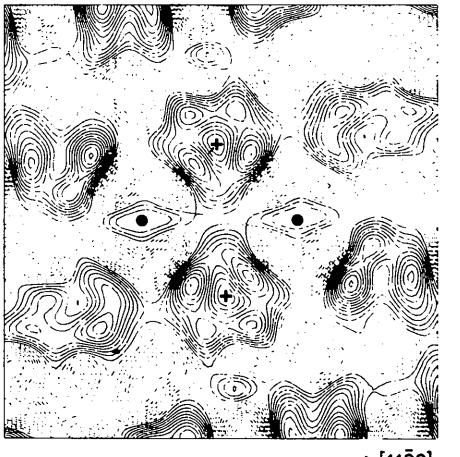

(*c*)

Fig. 2. The deformation density of V_2O_3 in (*a*) the (11$\bar{2}$0) section, (*b*) a section parallel to the basal plane at $z = \frac{1}{3}$, *i.e.* bisecting the 2·88 Å V′—V″ bond in Fig. 1 and (*c*) a section containing two O-atom (crosses) and two Ti-atom sites (filled circles), marked O, O′, Ti′ and Ti″ in Fig. 1. Contour intervals are at 0·02 e Å^{-3}. Negative contours are represented as dotted lines starting at 0·0 e Å^{-3}. The broken lines indicate the limits of the theoretical deformation-density map shown in Fig. 4.

accumulation of errors or perhaps as a deficiency in the method adopted here of calculating deformation densities), nonetheless the observed features in the vicinity of this bridge, and in particular that of the previously described three-leaf clover, are significant. In fact, an error plot across one of the electron-density lobes along [10$\bar{1}$0] shows that the peak density exceeds its error by a factor of about two.

The strong, irregularly shaped maxima between the metal-atom sites in the map of Fig. 2(*a*) belong to the O atoms. Their charge deformation can be studied in Fig. 2(*c*) which shows a section through the atomic sites O, O′, V′ and V″ (Fig. 1). It is plain that a charge accumulation occurs at the O atoms and that the maxima are located slightly off-centre in the direction of each nearest metal-atom site. The deformation density along the V′–O and O–V″ vectors and the corresponding error curves have been represented in Figs. 3(*d*) and 3(*e*). One can see that the bonding features along these two crystallographically non-equivalent but chemically equivalent directions are similar. Interestingly, they also resemble closely those which have been found along the corresponding directions in Ti_2O_3, except that in the latter compound

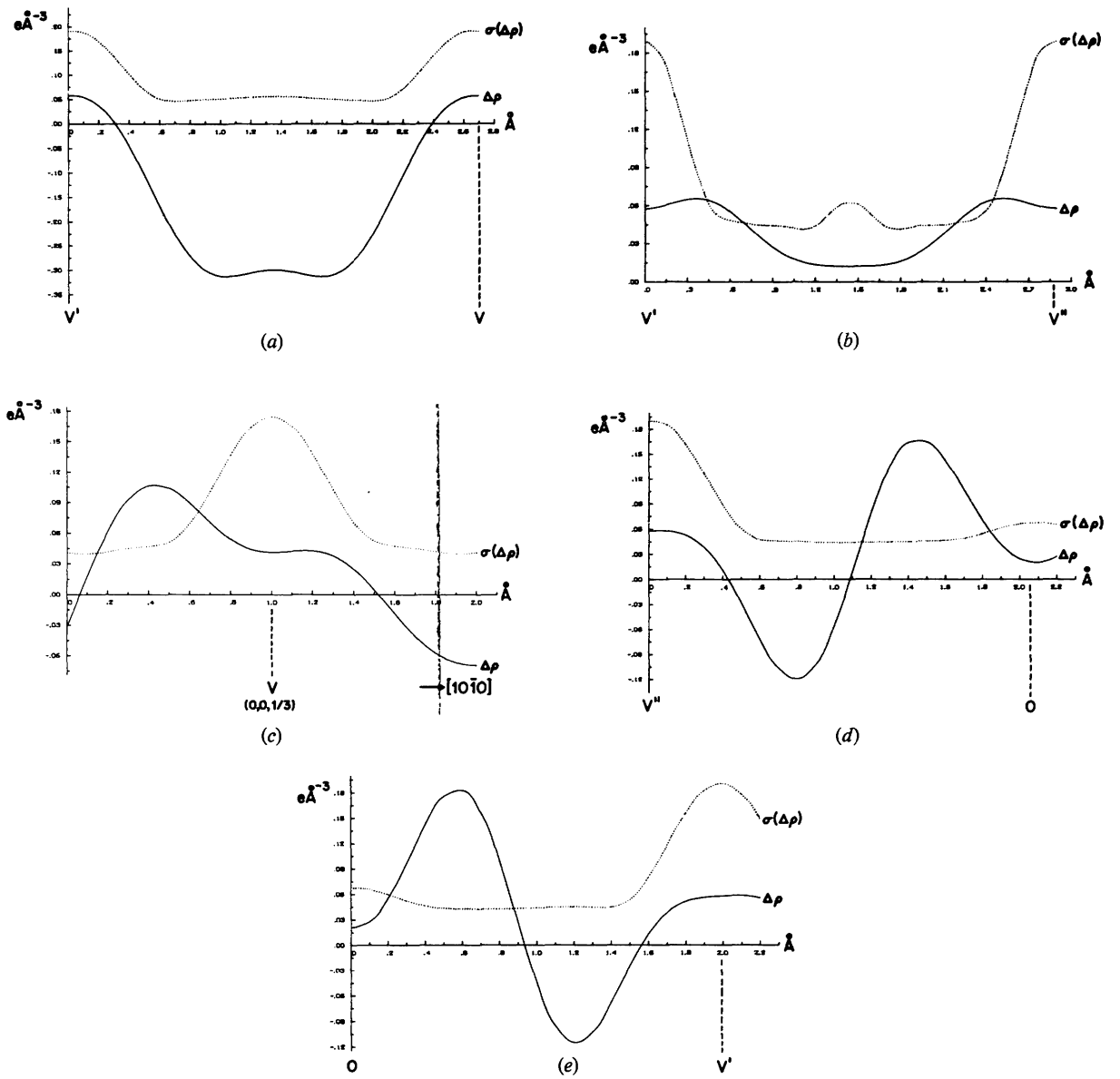

Fig. 3. The deformation density $\Delta\rho$ (solid line) and its error $\sigma(\Delta\rho)$ (dotted line) (*a*) along the V′–V vector, (*b*) along the V′–V″ vector, (*c*) through one of the deformation-density lobes along [10$\bar{1}$0] as shown in Fig. 2(*b*), (*d*) along the V″–O vector and (*e*) along the O–V′ vector.

the deformation density at the metal-atom site is negative (VYGA).

These observations can be interpreted as follows. An electron transfer occurs from the V to the O atoms which presumably leads to a filling of the O p states and leaves the V atoms in a d^2 configuration. However, due to covalency with the V d states the formal electric charges of the O^{2-} and V^{3+} ions are reduced with respect to the fully ionic values. The valence electrons remaining on the V atoms are available for the formation of metal–metal bonds. In view of the deformation of these atoms one can conclude that the bond orbitals occupied are mainly those which are directed away from the c axis, their orientation being such that they are bridging the metal–metal bond axes in the plane parallel to the basal plane. Thus the metal atoms interact mainly *via* π bonds across common edges of the O-atom octahedra. This situation is different to that found in Ti_2O_3 where they interact mainly *via* σ bonds across common faces of the O-atom octahedra.

Clearly these results are in accordance with theory and in particular with the schematic band structures proposed by Van Zandt, Honig & Goodenough (1968) and Goodenough (1971), and the theoretical band structures calculated by Ashkenazi & Weger (1976) and Ashkenazi & Chuchem (1975). According to these authors the energy levels of V_2O_3 at room temperature are arranged in such a way that the centre of gravity of the e_g^π band, which derives from the V d orbitals directed away from **c**, lies below that of an a_{1g} band, which derives from the V d orbitals directed parallel to **c**. Deformation-density maps calculated from these band structures are represented in Fig. 4. The first map shows a section of the $(11\bar{2}0)$ plane which is marked by broken lines in the corresponding experimental map of Fig. 2(*a*). One can see that the main features of the theoretical map, such as the deformation of the V atoms and the charge accumulation at the O atoms, are qualitatively reproduced by the experimental map. Major differences occur in the immediate vicinity of the metal-atom sites where the experimental map shows a positive (non-significant) deformation density, and around the O-atom sites where it shows a charge accumulation which deviates strongly from spherical symmetry. As will be discussed in more detail in a forthcoming article (Ashkenazi, Vincent, Yvon & Honig, 1980), the latter difference is probably related to the deficiencies of the model on which the calculation of the theoretical map has been based.

The second theoretical map in Fig. 4 shows the section parallel to the basal plane which is marked by broken lines in the corresponding experimental map of Fig. 2(*b*). The agreement between the two maps is fairly good. In particular, the positive deformation density lobes in the theoretical map which represent the metal e_g^π bond orbitals resemble closely the three-leaf clover-shaped maxima in the experimental map. The orientation of these lobes is the same in both maps, *i.e.* they are not pointing exactly toward the nearest metal-atom sites but are directed slightly above and below the edges of the O-atom octahedra.

In summary, the bonding features found in the present analysis and in that reported previously (VYGA) are consistent with theoretical predictions. They confirm the existence of metal–metal bonds across the faces (Ti_2O_3) and edges (V_2O_3) of the O-atom octahedra and explain why the c/a ratio of Ti_2O_3 is anomalously low and that of V_2O_3 is anomalously high. It is interesting to note that the

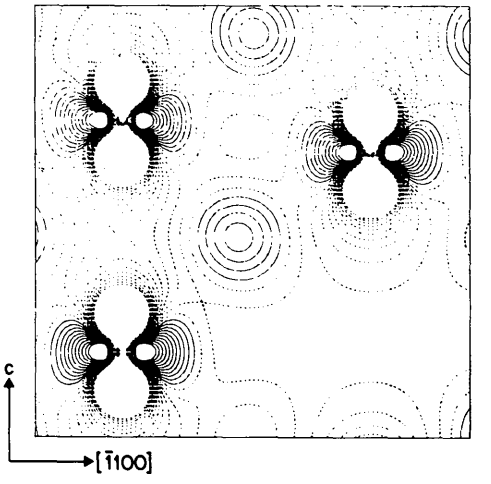

(*a*)

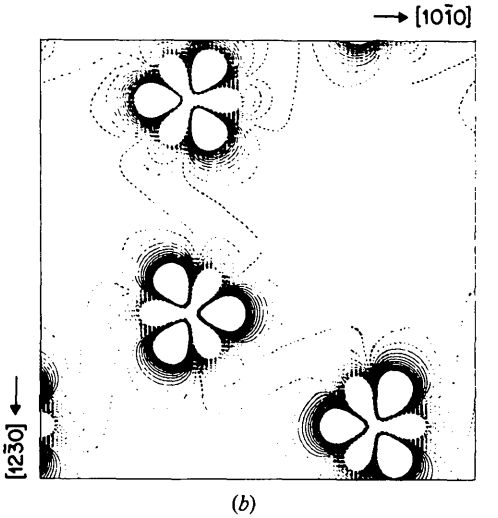

(*b*)

Fig. 4. The theoretical deformation density of V_2O_3 in (*a*) the $(11\bar{2}0)$ section and (*b*) a section parallel to the basal plane at $z = \frac{1}{3}$, according to Ashkenazi, Vincent, Yvon & Honig (1980). The corresponding regions in the experimental maps of Fig. 2 are marked by broken lines. Contour intervals are at 0·02 e Å^{-3}. Negative contours are represented as dotted lines starting at 0·0 e Å^{-3}. Contours beyond ±0·22 e Å^{-3} have been suppressed for clarity.

relative strength between these two types of metal–metal bonds is also reflected in the M—O lengths. Due to electrostatic repulsion the metal cations in these oxides are shifted away from the centre of the O-atom octahedra along **c** in such a way that the bond lengths between the metal atoms and the O atoms sharing an octahedral face are longer than those between the metal atoms and the O atoms not sharing an octahedral face (Fig. 1). Since their difference, Δd, is bigger in V_2O_3 ($\Delta d = 2{\cdot}05 - 1{\cdot}97 = 0{\cdot}08$ Å) than in Ti_2O_3 ($\Delta d = 2{\cdot}07 - 2{\cdot}03 = 0{\cdot}04$ Å), one can conclude that the metal–metal interactions across the octahedral faces, which counteract the electrostatic repulsion, are weaker in V_2O_3 than in Ti_2O_3.

Finally, it is worth mentioning that the experimentally determined electron-density maps of Ti_2O_3 and V_2O_3 as presented in this work show internal consistency as far as the bonding features around the O atoms are concerned. As can be seen from a comparison of the deformation maps shown in Fig. 5, the charge-density distribution in the vicinity of these atoms is remarkably similar in both compounds. This is not unexpected and may be taken as a testimony of the quality of the X-ray measurements and the method of structural refinement.

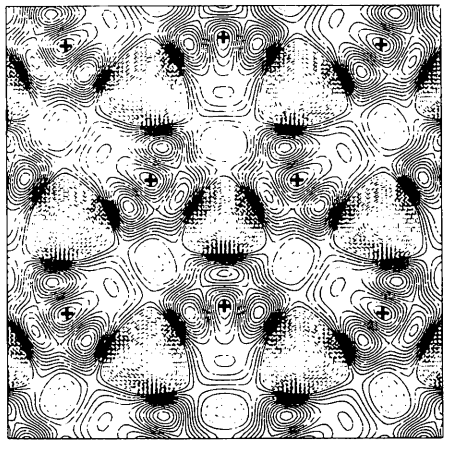

(*a*)

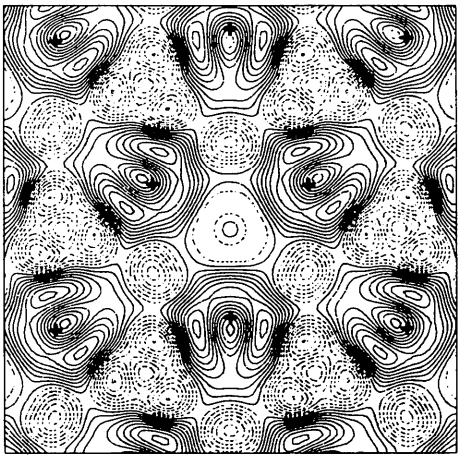

(*b*)

Fig. 5. A comparison of the deformation-density maps across a layer of O-atom sites perpendicular to **c** for (*a*) Ti_2O_3 and (*b*) V_2O_3. The O-atom sites are marked by crosses. Contour intervals are at 0·02 e Å^{-3}.

The authors thank Professor J. M. Honig for providing the V_2O_3 crystal. This work was supported in part by the Swiss National Science Foundation, grant No. 2.246-0.79.

References

ASHKENAZI, J. & CHUCHEM, T. (1975). *Philos. Mag.* **32**, 763–785.

ASHKENAZI, J., VINCENT, M. G., YVON, K. & HONIG, J. M. (1980). *Solid State Commun.* In the press.

ASHKENAZI, J. & WEGER, M. (1976). *J. Phys.* (*Paris*), **37**, 189–198.

BECKER, P. J. & COPPENS, P. (1974). *Acta Cryst.* A**30**, 129–153.

BECKER, P. J. & COPPENS, P. (1975). *Acta Cryst.* A**31**, 417–425.

CASTELLANI, C., NATOLI, C. R. & RANNINGER, J. (1978). *Phys. Rev. B*, **18**, 4967–5000.

CRUICKSHANK, D. W. J. (1949). *Acta Cryst.* **2**, 65–82.

DERNIER, P. D. (1970). *J. Phys. Chem. Solids*, **31**, 2569–2575.

DWIGGINS, C. W. (1975). *Acta Cryst.* A**31**, 395–396.

FLACK, H. D. & VINCENT, M. G. (1978). *Acta Cryst.* A**34**, 489–491.

FUKAMACHI, T. (1971). Tech. Rep. B12, Institute for Solid State Physics, Univ. of Tokyo.

GOODENOUGH, J. B. (1963). *Magnetism and the Chemical Bond.* New York: Interscience–John Wiley.

GOODENOUGH, J. B. (1970). *Proceedings of the Tenth International Conference of Physics of Semiconductors*, edited by S. D. KELLER, J. C. HENSEL & F. STERN, pp. 304–310. US Atomic Energy Commission.

GOODENOUGH, J. B. (1971). *Prog. Solid State Chem.* **5**, 145–399.

International Tables for X-ray Crystallography (1974). Vol. IV. Birmingham: Kynoch Press.

MCWHAN, D. B., RICE, T. M. & REMEIKA, J. P. (1969). *Phys. Rev. Lett.* **23**, 1384–1387.

PREWITT, C. T., SHANNON, R. D., ROGERS, D. B. & SLEIGHT, A. W. (1969). *Inorg. Chem.* **8**, 1985–1993.

REES, B. (1976). *Acta Cryst.* A**32**, 483–488.

REES, B. (1978). *Acta Cryst.* A**34**, 254–256.

THORNLEY, F. R. & NELMES, R. J. (1974). *Acta Cryst.* A**30**, 748–757.

VAN ZANDT, L. L., HONIG, J. M. & GOODENOUGH, J. B. (1968). *J. Appl. Phys.* **39**, 594–595.

VINCENT, M. G. & FLACK, H. D. (1979). *Acta Cryst.* A**35**, 78–82.

VINCENT, M. G., YVON, K., GRÜTTNER, A. & ASHKENAZI, J. (1980). *Acta Cryst.* A**36**, 803–808.

XRAY SYSTEM (1976). Tech. Rep. TR-446. Computer Science Center, Univ. of Maryland, College Park, Maryland.